blood

2013 122: 2743-2750
Prepublished online August 27, 2013;
doi:10.1182/blood-2013-05-501692

Human VKORC1 mutations cause variable degrees of 4-hydroxycoumarin resistance and affect putative warfarin binding interfaces

Katrin J. Czogalla, Arijit Biswas, Ann-Christin Wendeln, Philipp Westhofen, Clemens R. Müller, Matthias Watzka and Johannes Oldenburg

Blood (print ISSN 0006-4971, online ISSN 1528-0020), is published weekly by the American Society of Hematology, 2021 L St, NW, Suite 900, Washington DC 20036.

Regular Article

THROMBOSIS AND HEMOSTASIS

Human VKORC1 mutations cause variable degrees of 4-hydroxycoumarin resistance and affect putative warfarin binding interfaces

Katrin J. Czogalla, Arijit Biswas, Ann-Christin Wendeln, Philipp Westhofen, Clemens R. Müller, Matthias Watzka, and Johannes Oldenburg

Institute of Experimental Haematology and Transfusion Medicine, University Clinic Bonn, Bonn, Germany

Key Points

- In vitro analysis of VKORC1 mutations perfectly reflects patients' warfarin resistance phenotypes.
- In silico docking of warfarin on a VKORC1 model reveals a putative docking site in agreement with the locations of OACR-associated mutations.

Since the discovery of warfarin-sensitive vitamin K 2,3-epoxide reductase complex subunit 1 (VKORC1), 26 human VKORC1 (hVKORC1) missense mutations have been associated with oral anticoagulant resistance (OACR). Assessment of warfarin resistance using the "classical" dithiothreitol-driven vitamin K 2,3-epoxide reductase (VKOR) assay has not reflected clinical resistance phenotypes for most mutations. Here, we present half maximal inhibitory concentrations (IC_{50}) results for 21 further hVKORC1 mutations obtained using a recently validated cell-based assay (*J Thromb Haemost* 11(5):872). In contrast to results from the dithiothreitol-driven VKOR assay, all mutations exhibited basal VKOR activity and warfarin IC_{50} values that correspond well to patient OACR phenotypes. Thus, the present assay is useful for functional investigations of VKORC1 and oral anticoagulant inhibition of the vitamin K cycle. Additionally, we modeled hVKORC1 on the previously solved structure of a homologous bacterial enzyme and performed in silico docking of warfarin on this model. We identified one binding site delineated by 3 putative binding interfaces. These interfaces comprise linear sequences of the endoplasmic reticulum–lumenal loop (Ser52-Phe55) and the first (Leu22-Lys30) and fourth (Phe131-Thr137) transmembrane helices. All known OACR-associated hVKORC1 mutations are located in or around these putative interfaces, supporting our model. (*Blood*. 2013;122(15):2743-2750)

Introduction

Initially introduced as a rodenticide, warfarin became the first synthetic oral anticoagulant (OAC) for human use and eventually one of the most prescribed drugs world-wide even though its mechanism of action was only recently clarified. In the 1970s, vitamin K 2,3-epoxide (K>O), a metabolite of vitamin K that accumulates as a result of vitamin K 2,3-epoxide reductase complex subunit 1 (VKORC1) inhibition by warfarin, was discovered.[1] Furthermore, Bell and Matschiner's[1,2] experiments revealed that K>O possessed procoagulant activity that could be blocked by warfarin, the first direct evidence for vitamin K epoxide reductase activity (VKOR). However, cloning of the *VKORC1* gene encoding VKORC1 was not successful until 2004.[3,4] VKORC1 reduces K>O to the quinone form of vitamin K (K) and sequentially to vitamin K hydroquinone (KH_2). KH_2 is a substrate of the enzyme γ-glutamyl carboxylase, which modifies vitamin K-dependent proteins, including the coagulation factors II, VII, IX, and X, by γ-carboxylation of certain glutamic acid residues.[5] In this process, K>O is generated as a by-product that can be reduced again by VKORC1 to complete the vitamin K cycle. Inhibition of VKORC1 by 4-hydroxycoumarins, including warfarin, results in decreased availability of KH_2 for γ-glutamyl carboxylase and, subsequently, results in increased levels of noncarboxylated, inactive vitamin K-dependent protein coagulation factors. This anticoagulant effect of 4-hydroxycoumarins is widely used in prevention and therapy of arterial or venous thromboses. However, there are wide variations in therapeutic dosage due to interindividual variables such as age, gender, weight, and co-medications as well as pharmacogenetic and pharmacokinetic determinants. A major pharmacogenetic factor is a polymorphism in the promoter region of VKORC1 (*VKORC1:c.-1639 G>A*) that significantly impacts effective OAC dosage.[6,7] Furthermore, pharmacokinetics of warfarin is influenced by several polymorphisms of cytochrome P450 isoform 2C9, the primary enzyme responsible for metabolizing 4-hydroxycoumarins.[8] In rare cases, missense mutations in VKORC1 have been associated with OAC resistance (OACR), clinically defined as greatly elevated coumarin dosage requirements, or even complete resistance. Since 2004, 26 different OACR-associated missense mutations in human VKORC1 (hVKORC1) have been reported.[3,7,9-16] However, the molecular mechanism of OAC inhibition of VKORC1 and how mutations in this enzyme lead to OAC resistance are still unclear. Historically, investigations of wild-type and mutant hVKORC1 have relied on the "classical" in vitro dithiothreitol-driven VKOR assay to measure VKORC1 function and assess OAC inhibition.[17,18] However, the dithiothreitol-driven assay has shown only 4 of the known human

Submitted May 10, 2013; accepted August 17, 2013. Prepublished online as *Blood* First Edition paper, August 27, 2013; DOI 10.1182/blood-2013-05-501692.

The online version of this article contains a data supplement.

The publication costs of this article were defrayed in part by page charge payment. Therefore, and solely to indicate this fact, this article is hereby marked "advertisement" in accordance with 18 USC section 1734.

Table 1. Warfarin IC_{50} for hVKORC1 variants determined by cell culture-based and dithiothreitol-driven in vitro assays and compared with patient dosage phenotypes

hVKORC1 variant	Warfarin IC_{50} ± SEM (nM)*	Variant IC_{50}/wild-type IC_{50} ratio*	Mean patient dosage in HDT multiples [drug]†	Warfarin IC_{50} by dithiothreitol-driven VKOR assay
Wild-type	24.7 ± 3.6	1.0 ± 0.2	1.0 [W, P] (n = 77)	Warfarin-sensitive (by definition)
Ala26Pro	1224 ± 5.2	49.6 ± 0.1	>3.0 [W] (n = 1)	11.2-Fold increased Ki (IC_{50})‡
Ala26Thr	74 ± 7.5	3.0 ± 0.2	>2.0 [P] (n = 1)	Sensitive‡
Leu27Val	62 ± 10.1	2.5 ± 0.2	>3.0 [F], 1.0 [W] (n = 1)‖	Sensitive‡
His28Gln	72 ± 8.2	2.9 ± 0.2	3.5 [P] (n = 1)	Sensitive‡
Val29Leu	136 ± 3.3	5.5 ± 0.1	2.0 [W] (n = 1)	Absence of expression‡/sensitive§
Asp36Gly	78 ± 6.6	3.2 ± 0.2	3.0 [W] (n = 1)	Sensitive‡
Asp36Tyr	93 ± 19.4	3.8 ± 0.3	1.5-3.5 [W] (n = 10)	Sensitive‡
Val45Ala	152 ± 4.4	6.2 ± 0.1	>2.0 [W] (n = 1)	Sensitive‡/sensitive§
Ser52Leu	182 ± 8.9	7.4 ± 0.2	>3.0 [P] (n = 1)	Low VKOR activity, Ki (IC_{50})determination not possible‡
Ser52Trp	140 ± 23.0	5.7 ± 0.2	3.5 [P] (n = 1)	Low VKOR activity, Ki (IC_{50}) determination not possible‡
Val54Leu	112 ± 2.8	4.5 ± 0.1	1.5-5.5 [W] (n = 2)	4.6-Fold increased Ki (IC_{50})‡
Ser56Phe	167 ± 11.9	6.8 ± 0.2	>5.0 [P] (n = 1)	Sensitive‡
Arg58Gly	85 ± 7.8	3.4 ± 0.2	5.0 [W] (n = 1)	Sensitive‡/sensitive§
Trp59Arg	433 ± 5.0	17.5 ± 0.1	7.0 [P] (n = 1)	Low VKOR activity, Ki (IC_{50}) determination not possible‡
Trp59Cys	188 ± 8.4	7.6 ± 0.2	>3.5 [P] (n = 1)	Sensitive‡
Trp59Leu	1858 ± 4.8	75.2 ± 0.1	>5.0 [P] (n = 1)	Low VKOR activity, Ki (IC_{50}) determination not possible‡
Val66Gly	69 ± 5.7	2.8 ± 0.2	2.5 [P] (n = 1)	Low VKOR activity, Ki (IC_{50}) determination not possible‡
Val66Met	134 ± 7.3	5.4 ± 0.2	3.0-6.0 [W] (n = 7)	Low VKOR activity, Ki (IC_{50}) determination not possible‡
Gly71Ala	127 ± 6.3	5.1 ± 0.2	>2.0 [P] (n = 1)	Low VKOR activity, Ki (IC_{50}) determination not possible‡
Asn77Ser	131 ± 15.5	5.3 ± 0.2	>3.0 [P] (n = 1)	Low VKOR activity, Ki (IC_{50}) determination not possible‡
Asn77Tyr	96 ± 3.7	3.9 ± 0.2	3.5 [W] (n = 1)	Low VKOR activity, Ki (IC_{50}) determination not possible‡
Ile123Asn	209 ± 3.7	8.5 ± 0.1	>7.0 [P] (n = 1)	2.4-Fold increased Ki (IC_{50})‡
Leu128Arg	1226 ± 8.4	49.7 ± 0.1	>4.0-7.0 [W] (n = 5)	Low VKOR activity, Ki (IC_{50}) determination not possible‡/sensitive§
Tyr139His	113 ± 5.2	4.6 ± 0.2	>3.0 [W] (n = 1)	3.6-Fold increased Ki (IC_{50})‡
TYA → Leu-Ile-Val	361 ± 11.1	14.6 ± 0.1	—	—

[P], phenprocoumon; [W], warfarin.

*IC_{50} values determined by the cell-based assay method as cited in Fregin et al[18] used for the present study.

†Data from Figures 2 and 3 and supplemental Table 3 of Watzka et al. HDT is defined as the high-dosage threshold and is equivalent to the mean patient population dosage divided by the control group (homozygous wild-type *VKORC1* alleles with *VKORC1*:c.-1639GG haplotype) population mean OAC dosage for each drug, where the patient achieved stable anticoagulation with an international normalized ratio within the range 2.0-3.0. n, number of reported patients with mutation.[13]

‡Results from Hodroge et al, the study assumes that $K_i = IC_{50}$.[17]

§results calculated from data in Rost et al[1] by methods detailed in Fregin et al.[18] ‖patient had cytochrome P450 isoform 2C9*2*3 haplotype, which results in a reduced warfarin dosage requirement to achieve a stable, therapeutic international normalized ratio compared with patients with wild-type cytochrome P450 isoform 2C9*1*1 haplotype.

mutations (Table 1) to be warfarin resistant in vitro due to methodological shortcomings, as described by Bevans et al.[3,19-21] We recently developed a cell-based assay for evaluating VKORC1 function and its inhibition by warfarin. In this assay, human FIX is coexpressed with VKORC1 variants in HEK 293T cells, and secreted FIX activity is measured as a surrogate marker for VKORC1 function.[22]

In the present study, we have used this cell-based assay to investigate warfarin resistance for 21 OACR-associated hVKORC1 missense mutations not previously investigated by this method. We show that the in vitro cell-based assay results are in overall agreement with clinical phenotypes of patients harboring these mutations. In addition, we modeled the hVKORC1 molecular structure and warfarin docking, based on sequence similarity to a recently solved structure of a prokaryotic homolog enzyme.[23] The modeling reveals 3 putative warfarin binding interfaces in agreement with the locations of the OACR-associated mutations.

Methods

Construction of hVKORC1/hFIX mammalian expression vectors

The *hVKORC1* cDNA was cloned into multiple cloning site B, and *hFIX* cDNA into multiple cloning site A of the biscistronic pIRES vector (Clontech, Saint-Germain-en-Laye, France) by a restriction-free cloning polymerase chain reaction protocol using Phusion DNA polymerase (Finnzymes, Vantaa, Finland).[24] *VKORC1* mutations were introduced in the h*VKORC1* cDNA by site-directed mutagenesis using PFU-Turbo-polymerase (Agilent Technologies, Böblingen, Germany). See supplemental Information for mutagenesis primers available on the *Blood* Web site.

Measurement of warfarin resistance

To assess relative warfarin sensitivities of wild-type and variant hVKORC1, we used the HEK 293T cell culture-based assay of Fregin et al.[22] In brief, activated FIX secreted into the cell culture medium is quantitated to serve as a surrogate measure of coexpressed VKORC1 activity in the absence or presence of warfarin at various concentrations (0, 0.01, 0.025, 0.05, 0.1, 0.25, 0.5, and 1 μM). FIX activity of filtered cell culture supernatants was measured using an Electra 1400c coagulometer (Instrumentation Laboratory, Munich, Germany) with activated partial thromboplastin reagent (aPTT SP; Instrumentation Laboratory) and FIX-deficient plasma (Helena-Biosciences, Gateshead, UK). Statistical analyses of raw dose-response data were performed using KaleidaGraph 4.04. Replicate measurements ($3 \leq n \leq 6$) were made of FIX activity in cell culture supernatants and mean value and SEM were calculated for all replicate data. A nonlinear least-squares curve-fitting procedure was used to obtain warfarin half maximal inhibitory concentrations (IC_{50}) values from the raw dose-response data (Figure 1). As a liberal estimate of the SEM for each respective IC_{50} value in Table 1, we applied the largest SEM value for the triplicate normalized FIX activities measured for all of the warfarin concentrations (ie, corresponding to the largest error bar for each dose-response curve shown in Figure 1). Accordingly, the SEM for each (variant IC_{50}/wild-type IC_{50}) ratio in Table 1 was calculated as follows: $SEM_{IC\ 50ratio} = \sqrt{\left(\frac{SEM_{IC\ 50var.\ iant}}{IC_{50var\ iant}}\right)^2 + \left(\frac{SEM_{IC\ 50wildtype}}{IC_{50wildtype}}\right)^2}$.

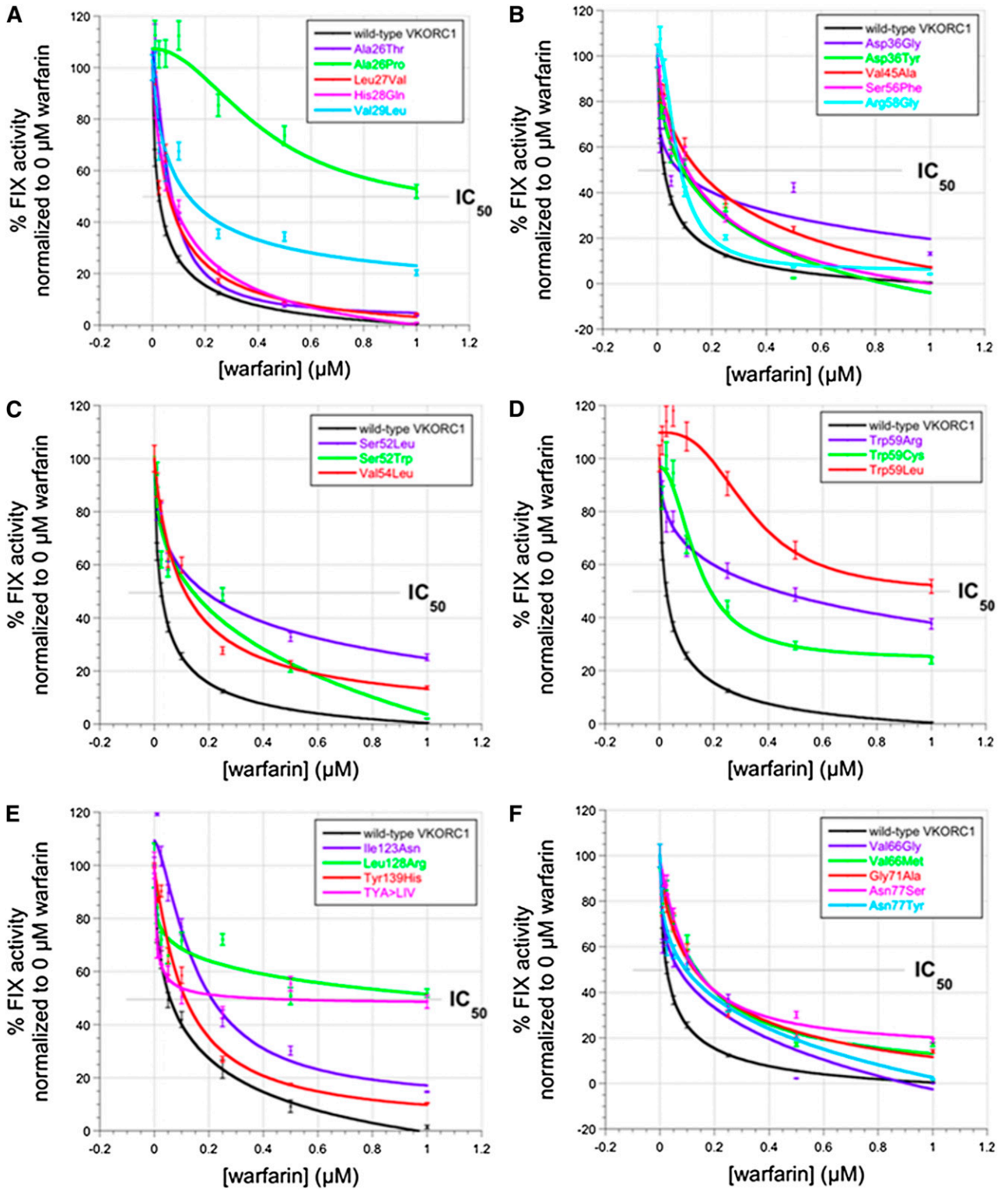

Figure 1. Dose-response curves for hVKORC1 variants measured by the cell culture-based assay. (A-F) Secreted FIX activity data for HEK 293T cells coexpressing FIX together with human wild-type or OACR-associated VKORC1 variants in the presence of various warfarin concentrations (0.00-1.0 μM). Data are mean values for n = 6 measurements and error bars show ±SEM. Data points and fitted curves for hVKORC1 wild-type and missense variants are color-coded according to the legend key in each panel.

In fact, average errors for our data were considerably less than this value (see error bars for each dose-response curve in Figure 1).

Assessment of VKORC1 protein expression

Relative VKORC1 variant expression levels in HEK 293T cells were determined by cloning the variant cDNAs into pcDNA3.1/myc-His expression vector (Life Technologies, Darmstadt, Germany).[24] Cells were lysed after 72-hour expression and VKORC1 variants quantitated by densitometry of immunostained western blots (see supplemental Information for detailed methods). hVKORC1 variants were detected using a polyclonal anti–C-Myc antibody (Sigma-Aldrich Chemie GmbH, Munich, Germany) and were normalized to constitutively expressed ERGIC-53 that was detected by

stripping western blots after hVKORC1 immunostaining and reprobing using an anti–ERGIC-53 antibody (ER-Golgi intermediate compartment; Santa Cruz Biotechnology, Inc., Heidelberg, Germany).[22]

Molecular modeling of hVKORC1 and in silico docking of warfarin on hVKORC1 model

A model of VKORC1 was constructed by comparative methods based on the X-ray crystal structure of the bacterial homolog (*Synechococcus* sp.) of VKORC1 (PDB ID: 3KP9) (http://www.pdb.org/pdb/home/home.do accessed on 12.09.2012) at 3.6 Å resolution using the YASARA (version 12.9.27, 1993-2011 by Elmar Krieger) homology modeling program.[23] Because VKORC1 is a transmembrane protein, membrane-embedded simulations were calculated for 10 nanoseconds in a phosphatidylcholine bilayer using YASARA. Docking of the anionic open-chain warfarin structure on the resulting hVKORC1 structure was performed using the AutoDock (1989-2013 by The Scripps Research Institute) implementation included in YASARA.[25-28] A rigid, global rolling ball search was performed using stationary VKORC1 and translating/rotating the warfarin structure. The generated interactions from the global search were analyzed using constraints of 2 critical disulfide bonds (Cys43-Cys51 and Cys132-Cys135). The best model was chosen on the basis of pseudo-energy scoring. A detailed description of the modeling and docking methods is presented in the supplemental Information.

Results

All hVKORC1 missense variants investigated show in vitro warfarin resistance by the cell culture-based assay

In the present study, we investigated 21 OACR-associated VKORC1 missense mutations according to the cell culture-based assay conditions recently published by our group. Measured protein expression levels for all VKORC1 variants studied here range from onefold to >fivefold of the wild-type expression level (supplemental Figure 1; supplemental Information).[22]

We further determined in vitro cell culture-based warfarin IC_{50} values for the 21 OACR-associated missense hVKORC1 variants. All mutations investigated by our assay exhibit warfarin dose-response data shifted to greater values than those for wild-type hVKORC1 at warfarin concentrations of 0 to 1 μM (Figure 1). These results confirm that the present assay accurately reports data that are in agreement with the clinical human warfarin-resistance phenotypes (Table 1). To summarize the dose-response data, we calculated the IC_{50} of warfarin for each hVKORC1 variant by standard curve-fitting methods (Table 1). These data allow us to classify the OACR mutations into mild, moderate, severe, or complete in vitro resistance phenotypes (mild: IC_{50} <100 nM; moderate: IC_{50} 100-200 nM; severe: IC_{50} 200-350 nM; complete: IC_{50} >350 nM). We further calculated relative increases in measured in vitro warfarin IC_{50} values by normalizing to the wild-type value of 24.7 nM (Table 1, column 3). All mutations assessed by the cell-based assay exhibited increases in IC_{50} over a range of between 2.5-fold and 8.5-fold, reflecting clinical OACR phenotypes that range from moderate to severe resistance. However, 4 mutations conferred greatly elevated IC_{50} values (Tp59Arg: 17.5-fold; Ala26Pro and Leu128Ag: 50-fold; Trp59Leu: 75-fold increases over wild-type IC_{50}), suggesting that patients with these VKORC1 variants exhibit complete warfarin resistance. Interestingly, most of the VKORC1 missense variants are associated with residual secreted FIX activities in the 0% to 40% range at 1 μM warfarin, whereas the 4 completely resistant variants exhibit residual activities of >50% at the same warfarin concentration. Thus, residual FIX activity at 1 μM applied warfarin appears to be equally predictive as IC_{50} value for distinguishing between moderate-to-severe and complete warfarin resistance.

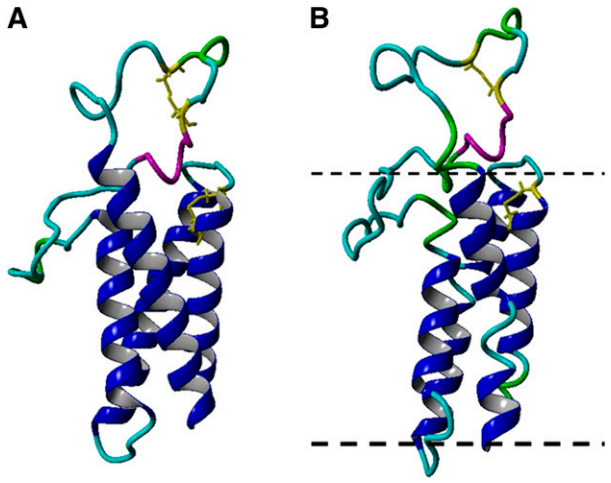

Figure 2. Molecular model of hVKORC1. (A) A backbone ribbon model of hVKORC1. Colors differentiate secondary structure elements, including transmembrane α-helices (blue), random coil (cyan), turn (green), and 1/2-helical segment (magenta). Conserved cysteine residue side-chains shown as yellow stick representations. (B) The simulation snapshot of the membrane-embedded structure of hVKORC1.

Mutagenesis of Thr138-Tyr139-Ala140 causes complete warfarin resistance in vitro

To investigate the role of the TYA motif (hVKORC1 residues 138-140) as a putative warfarin binding site in hVKORC1, we mutated the tripeptide to Leu-Ile-Val.[5,29-31] In our in vitro assay, this VKORC1 variant exhibits a complete warfarin resistance, suggesting that the TYA motif forms a structural requirement for warfarin inhibition (Table 1, 14.6-fold greater IC_{50} than wild-type; Figure 1E, residual FIX activity of 50% at 1 μM warfarin).

The hVKORC1 structural model characteristics

In accordance with the template structure, our homology-based hVKORC1 model comprises of similar secondary structural elements and overall protein fold.[23] Our hVKORC1 model is a 4 transmembrane α-helix (TM1-4) bundle structure (supplemental Table 1) with a long periplasmatic surface loop between TM1 and TM2 (Ala32-Ser79; for detailed validation, see supplemental Information). Like the bacterial homolog, our model consists of a highly conserved serine-rich helical segment (Ser52-Ser57) in hVKORC1 (Figure 2). The threonine, tyrosine, alanine (TYA) motif implicated in warfarin binding in previous studies forms part of the fourth trans-membrane α-helix and is deep within the membrane bilayer. The conserved cysteine pairs, Cys43-Cys51 and Cys132-Cys135, are located in the cytoplasmic loop and the fourth trans-membrane α-helix (Figure 2).

Docking of warfarin to the homology model identifies putative binding surfaces

We used the molecular model of hVKORC1 to investigate possible warfarin binding sites by in silico molecular docking. Results from a previous in vitro structure-activity study revealed that the open side-chain conformation of anionic racemic warfarin is the active inhibitory isomer.[32] An initial coarse-grained rolling ball docking search using the anionic (deprotonated) open side-chain form of *R*-warfarin yielded 12 interaction geometries (supplemental Figure 5; supplemental Information). Visual inspection of the docked structures revealed 3 distinct regions of docked warfarin: the cytoplasmic

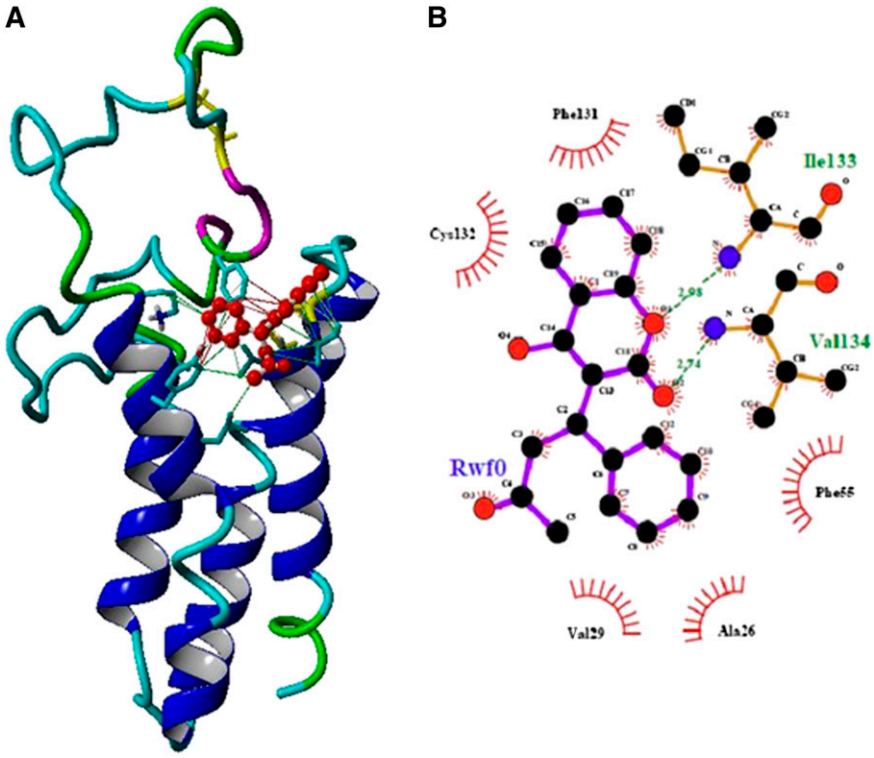

Figure 3. Docking of warfarin to the homology modeled hVKORC1 structure. (A) A ribbon diagram of the hVKORC1 homology model with docked warfarin depicted as red balls. Interactions between warfarin and hVKORC1 interface residues are represented as solid lines (hydrophobic and π-interactions). (B) A ligplot representation of the interactions between warfarin and amino acid residues of hVKORC1. Hydrogen bonds are indicated by dotted lines and hydrophobic contacts are represented by arcs with spokes radiating toward the contact atoms.

aqueous/endoplasmic reticulum (ER) membrane interface (supplemental Figure 5A), the protein/lipid bilayer interface (supplemental Figure 5B), and the ER lumenal loop (supplemental Figure 5C). We chose to further investigate one docking position with the highest ranked pseudo-energy score (supplemental Figure 5 [warfarin molecule colored red]; Figure 3). This position is proximal to the loop cysteines and the CXXC motif. Based on this position, we could define 3 molecular surfaces on hVKORC1 that represent putative interaction interfaces for warfarin: (1) the ER end of the first transmembrane helix (Leu22–Lys30); (2) a face of the serine-rich helix (Ser52-Phe55); and (3) a segment of the fourth transmembrane helix continuing into the large ER loop (Phe131-Thr137) (Figures 3 and 4; Table 2). The TYA motif is in proximity to the third predicted interface (Phe131-Thr137) and therefore may be critical to the structural integrity of the binding pocket. Interestingly, all known 4-hydroxycoumarin resistant mutations are found clustered around these 3 putative interfaces. Except for Tyr139, all mutations affect residues predicted to be in the polar lipid head-group region of the ER membrane leaflet or on the ER lumen-exposed loop.

Discussion

In our present study, we demonstrate for the first time in vitro expression and IC_{50} data for 21 OACR-associated hVKORC1

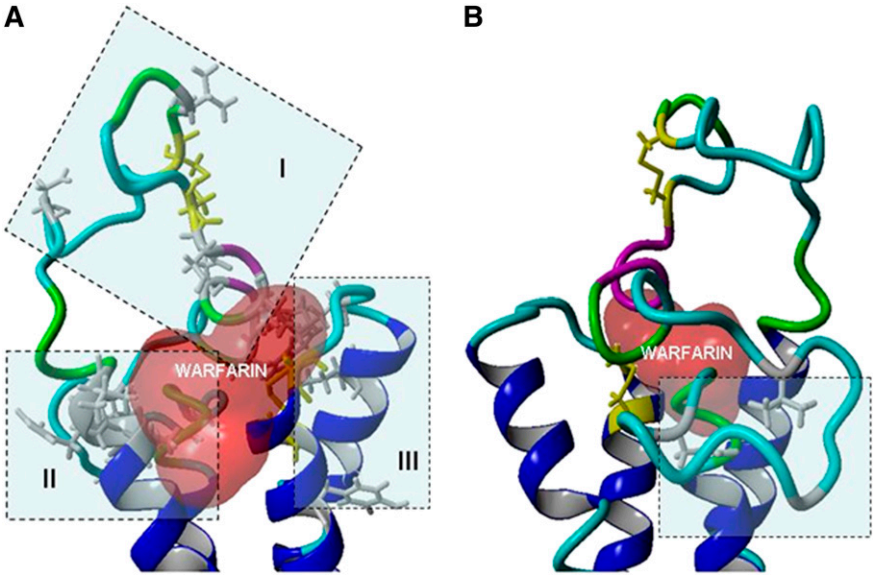

Figure 4. Binding interfaces for warfarin on hVKORC1 in relation to OACR mutations. (A) A close-up view of the 3 putative wafarin binding interfaces of hVKORC1 for the position with the best pseudo-energy docking score. The putative warfarin binding interfaces are highlighted by blue boxes and identified by roman numerals; (I), (II) and (III) indicate the first, second, and third binding interfaces, respectively. Reported human mutations influencing each interface are depicted as stick diagrams in gray color. The conserved loop and CXXC motif cysteine residues are represented in yellow stick form. The protein backbone is depicted in ribbon format. The warfarin molecule is represented by its solvent accessible surface area (colored red). (B) The horizontally opposite view of panel A showing the mutations (in blue box) that are distant to the 3 putative binding interfaces located in the membrane embedded segment of the loop.

Table 2. Warfarin binding interfaces on hVKORC1

Warfarin binding interface	Corresponding hVKORC1 residues	Mutations associated with binding interface
I	Leu22-Val29	Ala26Thr, Ala26Pro, Leu27Val, His28Gln, Val29Leu
II	Ser52-Phe55	Ser52Leu, Ser52Trp, Val54Leu, Asp36Gly, Asp36Tyr, Val45Ala, Ser56Phe, Arg58Gly Trp59Arg, Trp59Cys, Trp59Leu
III	Phe131-Thr137	Leu128Arg, Ile123Asn, Tyr139His
Membrane embedded loop segment	Gly62-Ser79	Val66Gly, Val66Met, Gly71Ala, Asn77Ser, Asn77Tyr

The 3 predicted interfaces for warfarin binding in VKORC1 (called interface I, II, and III) are listed here along with the residues/reported mutations that are located close to each of these interfaces and the 5 mutations that are distant to the 3 interfaces.

mutations in addition to the 3 previously reported variants in Fregin et al[15,22] that are in excellent agreement with the reported phenotypes for patients harboring the respective mutations. These data allow us to rank the severity of the mutations as moderate to severe or complete warfarin resistance. Furthermore, we simulated warfarin binding on a structural model of hVKORC1 and identified putative warfarin binding interfaces consistent with locations of known OACR-associated VKORC1 mutations.

Warfarin interaction with hVKORC1

Evolutionarily, VKORC1 is an ancient enzyme that is also found in bacterial and archaeal genomes. The crystal structure of a bacterial homolog of VKORC1 (*Synechococcus* sp.) shows that it comprises 5 TMs (PDB ID:3KP9).[23] The first 4 α-helices form the VKOR protein core domain (Pfam family *VKOR* PF07884). The fifth TM is a prokaryotic-specific extension that results in placement of a fused thioredoxin (Trx)-like on the periplasmic side of the membrane and is lacking in mammalian VKOR homologs. Our hVKORC1 homology model is based on the available crystal structure of *Synechococcus* VKOR on which application of a direct primary sequence alignment provides support for the 4TM topology choice.[23] Accordingly, for the 4TM model, the loop between the first and second TM α-helices is predicted to be located in the ER lumen. This topology is also supported by previously published experimental results for electron transfer from the conserved loop cysteines Cys43 and Cys51 to the CXXC motif in the fourth TM α-helix.[20,23,33,34] This electron transfer is essential for in vivo VKOR activity. Further experimental support for the 4TM topology model is provided by studies demonstrating that various ER lumenal oxidoreductase proteins interact with the loop cysteines of hVKORC1.[35] However, Tie et al[36,37] recently demonstrated in a VKORC1 and VKORC1L1 double knock-out cell line with their cell-based assay that Cys51, as well as in combination with Cys43, is not required for VKOR activity. Only the Cys43 is necessary to maintain VKOR activity. These data are seen as further support for the 3TM topology model in which the loop cysteines are located in the cytoplasm and are not required for electron transfer for active site regeneration after each cycle of oxidation. Thus, the membrane topology of hVKORC1 is still unclear, and currently there is a debate existing whether hVKORC1 comprises 3 or 4 joined transmembrane α-helices.[15,20,23,35,36,38] A recent review by Van Horn[39] comprehensively discusses the current experimental evidence for both models.

The clustering of OACR-associated mutations chiefly in the ER lumenal loop and the adjacent ends of the transmembrane helices suggests that warfarin may bind in this region of hVKORC1.[20,23,33] Our in silico warfarin docking results support this hypothesis, because the most favorable docking pseudo-energy scores were associated with this region. We have identified 3 discontiguous putative warfarin binding interfaces that are located in the ER lumenal loop and adjacent regions of TM1 and TM4 (Figure 3 and 4; Table 2). Accordingly, all human OACR-associated VKORC1 mutations are located in or near to these interfaces, suggesting they influence the interaction of warfarin with hVKORC1. Warfarin binding might inhibit hVKORC1 activity in 3 possible ways: (1) binding of warfarin may sterically hinder the reduction of the disulphide bridge between Cys43 and Cys51 in the ER luminal loop by physiological redox partners (eg, protein disulfide isomerase or other Trx-domain oxidoreductases); (2) warfarin binding might disturb the electron transfer to the CXXC motif, the catalytically active center of VKORC1; or (3) warfarin might physically block access of K>O to the substrate binding pocket adjacent to the CXXC motif.

Mutations located at the first putative warfarin binding interface

The residues Leu22-Lys30 comprise the first putative warfarin binding interface. In total, there are 5 human OACR-associated VKORC1 mutations within this interface (Ala26Thr, Ala26Pro, Leu27Val, His28Gln, and Val29Leu) (Figure 4A; Table 2). The most severe warfarin resistance phenotype among these residues is associated with the Ala26Pro substitution (IC_{50} of 1224.0 nM) (Table 1; Figure 1A). The substitution of alanine to a proline residue is predicted to break the natural helical conformation in this region and might induce major conformational changes to the putative warfarin binding site. However, the substitution of alanine to threonine resulted in only a mild resistance phenotype. Unlike alanine, threonine is a hydrogen bond donor and may have an influence on warfarin binding. The 3 other OACR-associated mutations in this region (His28Gln, Leu27Val, Val29Leu) also result in mild to moderate warfarin resistance (Table 1; Figure 1A). Of these substitutions, the first involves the exchange of a charged for a neutral side chain, although both can form hydrogen bonds. The second and third variants are conservative substitutions involving aliphatic, hydrophobic side chains.

Mutations at the second putative warfarin binding interface

The second putative warfarin binding interface is located between Ser52 and Phe55. There are 3 mutations located within this interface (Ser52Leu, Ser52Trp, Val54Leu) and 8 more mutations that are in close proximity (Figure 4A; Table 2). This interface is part of the amphipathic highly conserved, serine-rich helix, which seems to be a common feature of VKOR in different species.[23] Mutations causing 4-hydroxycoumarin resistance located at this interface generally exhibit a moderate warfarin resistance phenotype. Interestingly, 3 of 4 mutations affect serine residues (Ser52Leu, Ser52Trp, Ser56Phe). These substitutions reflect physiochemically nonconservative changes. Furthermore, these substitutions would disrupt any potential polar interactions with warfarin. Two further mutations are in close proximity to this interface. The Arg58Gly substitution might alter electrostatic potential and surface accessibility affecting warfarin binding. Mutations of Trp59 result in an ~8- to 75-fold increase of in vitro measured IC_{50} corresponding to moderate to complete in vivo warfarin resistance depending on the specific

substitution (Table 1, cf Trp59Arg, Trp59Cys, Trp59Leu). We are tempted to speculate that complete resistance implicates Trp59 as a crucial residue for warfarin binding, possibly having physical contact with bound warfarin. Although our model suggests that Arg58 does not participate in any contacts with neighboring residues, Trp59 forms hydrogen bonds with Tyr119 from TM3 and Gln78 and/or Asn80 on TM2. Additionally, Trp59 may have hydrophobic interactions with nearby Leu128, Val127, and Ile123. This network of potential interactions may allow Trp59 to act as a hinge for conformational rearrangements of the flexible loop (supplemental Figure 6). This fits with the suggestion by Li et al[23] that Trp59 may serve as an "anchor" of the serine-rich 1/2-helix of the ER lumenal loop. Although in our model, Trp59 is not located directly at a warfarin binding-VKORC1 interface, we hypothesize that mutations at Trp59 influence the movement of the serine-rich helix during electron transfer from Cys43 and Cys51 to Cys132 and Cys135 of the active site CXXC motif. Thus, these results suggest that the serine-rich helix in the periplasmatic ER lumenal loop represents a structure crucial to hVKORC1 protein function and warfarin binding. Three other variants on the outer surface loop exhibit a moderate in vitro resistance phenotype (Asp36Gly, Asp36Tyr, and Val45Ala). These 3 mutations might alter the conformation of the surface loop and affect conformational elements of the second putative warfarin binding interface.

Mutations at the third putative warfarin binding interface

The third putative warfarin interaction interface is located between TM3 and TM4 as well as in the ER lumenal end of TM4 (Phe131-Thr137) (Figure 4A; Table 2). The Leu128Arg mutation is located at the edge of this interface. The Leu128 residue is the first of the TM4 helix, and its side chain partly faces Ser57 in the serine-rich helix of the second interface. The introduction of the large, positively charged Arg side chain may lead to clashes with the neighboring residues and result in conformational changes within the third interface. The variant Leu128Arg might also alter the second putative interface because of its potential interaction with Trp59 (see previous section). The mutation Leu128Arg exhibits one of the most severe warfarin-resistant phenotypes (IC_{50} of 1123.9 nM) (Figure 1E). The Ile123Asn substitution is located at the end of TM3, adjacent to the third putative warfarin binding interface. The mutation to an Asn residue results in a change in polarity. Also, the potential interaction between Leu128 and Trp59 might be affected. Tyr139His is also located close to this putative interface. The Tyr139 residue is at the center of the TYA motif assigned in earlier studies as an important motif for dicoumarol binding in NQO1 (DT-diaphorase), a membrane-associated enzyme that reduces menadione (vitamin K_3).[40] The TYA motif in our model is not a direct part of the putative third interface but is adjacent to it. The residues from this motif are positioned to participate in intra-helical hydrogen bonds with the neighboring Cys135 of the active site CXXC motif as well as with the other residues from the third interface (supplemental Figure 7). There is only one human mutation affecting the TYA motif, Tyr139His, that exhibits a moderate resistance phenotype by our cell-based assay (IC_{50} of 113.1 nM) (Table 1; Figure 1E). To further investigate the role of the TYA motif in warfarin binding, we mutated the whole motif to Leu-Ile-Val. We chose these amino acids as conservative substitutes for the wild-type residues with aliphatic side chains. In our in vitro assay, the completely mutated TYA motif exhibits complete warfarin resistance (IC_{50} of 360.7 nM) (Table 1; Figure 1E). This result suggests that the TYA motif is indirectly involved in warfarin binding.

Mutations distant from all 3 putative warfarin binding interfaces

There are 5 mutations associated with in vivo warfarin resistance in human patients that are not in proximity to the putative warfarin binding interfaces (Val66Gly, Val66Met, Gly71Ala, Asn77Ser, and Asn77Tyr) (Figure 4B; Table 2). These mutations are located within a segment of the ER lumenal loop between TM1 and TM2 that potentially interacts with the surrounding lipid bilayer. Except for Val66Gly and Asn77Tyr that result in a mild resistance, all other mutations exhibit moderate resistance phenotypes. These mutations reflect semiconservative physiochemical changes with respect to the respective wild-type residues. Therefore, these mutations might induce minor changes in the conformation of the embedded portion of the loop and possibly affect the second putative warfarin binding interface.

In conclusion, our combined in vitro and in silico investigations of 21 OACR-associated hVKORC1 missense mutations reveal their respective mechanisms of action. In contrast to previously published in vitro data, the expression data for our study indicate wild-type or greater than wild-type expression levels for all variants expressed in HEK 293T cells.[19] In vitro measurements of warfarin inhibition of hVKORC1 variants allow us to classify the mutations as mild, moderate, severe, or complete in vitro resistance phenotypes. Additionally, the calculated mutant/wild-type IC_{50} ratios are good approximations of the increased therapeutic 4-hydroxycoumarin dosage requirements for patients with the respective OACR mutations. The clustering of the OACR-associated mutations in the ER lumenal loop as well as in adjacent transmembrane α-helices suggests that these regions are important for warfarin binding. Accordingly, in silico docking studies revealed 3 putative warfarin binding interfaces for hVKORC1 harboring almost all of the 26 known OACR-associated hVKORC1 missense mutations.

Given the overall success of the current assay in revealing in vitro warfarin resistance phenotypes for the hVKORC1 missense mutations, this assay might represent a helpful tool for guidance of dosages in patients with these and still unknown mutations in hVKORC1. Furthermore, the assay can be used to probe the influence of any intracellular modulator of hVKORC1 enzymatic activity and thus represents an important tool for future investigations of VKORC1 function.

Acknowledgments

This work was supported, in part, by funding from Baxter Germany GmbH (to J.O.) and from the Deutsche Forschungsgemeinschaft grant Ol100 5-1 (to M.W. and J.O.).

Authorship

Contribution: K.J.C., P.W., C.R.M., M.W., and J.O. designed the experiments; K.J.C. and A.-C.W. collected the data; K.J.C., A.B., M.W., and J.O. analyzed the data and produced the figures; A.B. was responsible for protein modeling and warfarin docking studies; and K.J.C., C.R.M., M.W., A.B., and J.O. drafted and edited the manuscript.

Conflict-of-interest disclosure: The authors declare no competing financial interests.

Correspondence: Johannes Oldenburg, Institute of Experimental Haematology and Transfusion Medicine, University Clinic Bonn, Sigmund-Freud Str 25, 53105 Bonn, Germany; e-mail: johannes.oldenburg@ukb.uni-bonn.de.

References

1. Bell RG, Matschiner JT. Vitamin K activity of phylloquinone oxide. *Arch Biochem Biophys.* 1970;141(2):473-476.
2. Bell RG, Matschiner JT. Warfarin and the inhibition of vitamin K activity by an oxide metabolite. *Nature.* 1972;237(5349):32-33.
3. Rost S, Fregin A, Ivaskevicius V, et al. Mutations in VKORC1 cause warfarin resistance and multiple coagulation factor deficiency type 2. *Nature.* 2004;427(6974):537-541.
4. Li T, Chang CY, Jin DY, Lin PJ, Khvorova A, Stafford DW. Identification of the gene for vitamin K epoxide reductase. *Nature.* 2004;427(6974): 541-544.
5. Oldenburg J, Bevans CG, Müller CR, Watzka M. Vitamin K epoxide reductase complex subunit 1 (VKORC1): the key protein of the vitamin K cycle. *Antioxid Redox Signal.* 2006;8(3-4):347-353.
6. Geisen C, Watzka M, Sittinger K, et al. VKORC1 haplotypes and their impact on the inter-individual and inter-ethnical variability of oral anticoagulation. *Thromb Haemost.* 2005;94(4): 773-779.
7. Rieder MJ, Reiner AP, Gage BF, et al. Effect of VKORC1 haplotypes on transcriptional regulation and warfarin dose. *N Engl J Med.* 2005;352(22): 2285-2293.
8. Oldenburg J, Bevans CG, Fregin A, Geisen C, Müller-Reible C, Watzka M. Current pharmacogenetic developments in oral anticoagulation therapy: the influence of variant VKORC1 and CYP2C9 alleles. *Thromb Haemost.* 2007;98(3):570-578.
9. Harrington DJ, Underwood S, Morse C, Shearer MJ, Tuddenham EG, Mumford AD. Pharmacodynamic resistance to warfarin associated with a Val66Met substitution in vitamin K epoxide reductase complex subunit 1. *Thromb Haemost.* 2005;93(1):23-26.
10. D'Ambrosio RL, D'Andrea G, Cafolla A, Faillace F, Margaglione M. A new vitamin K epoxide reductase complex subunit-1 (VKORC1) mutation in a patient with decreased stability of CYP2C9 enzyme. *J Thromb Haemost.* 2007;5(1):191-193.
11. Wilms EB, Touw DJ, Conemans JM, Veldkamp R, Hermans M. A new VKORC1 allelic variant (p.Trp59Arg) in a patient with partial resistance to acenocoumarol and phenprocoumon. *J Thromb Haemost.* 2008;6(7):1224-1226.
12. Bodin L, Perdu J, Diry M, Horellou MH, Loriot MA. Multiple genetic alterations in vitamin K epoxide reductase complex subunit 1 gene (VKORC1) can explain the high dose requirement during oral anticoagulation in humans. *J Thromb Haemost.* 2008;6(8):1436-1439.
13. Peoc'h K, Pruvot S, Gourmel C, dit Sollier CB, Drouet L. A new VKORC1 mutation leading to an isolated resistance to fluindione. *Br J Haematol.* 2009;145(6):841-843.
14. Schmeits PC, Hermans MH, van Geest-Daalderop JH, Poodt J, de Sauvage Nolting PR, Conemans JM. VKORC1 mutations in patients with partial resistance to phenprocoumon. *Br J Haematol.* 2010;148(6):955-957.
15. Watzka M, Geisen C, Bevans CG, et al. Thirteen novel VKORC1 mutations associated with oral anticoagulant resistance: insights into improved patient diagnosis and treatment. *J Thromb Haemost.* 2011;9(1):109-118.
16. Harrington DJ, Siddiq S, Allford SL, Shearer MJ, Mumford AD. More on: endoplasmic reticulum loop VKORC1 substitutions cause warfarin resistance but do not diminish gamma-carboxylation of the vitamin K-dependent coagulation factors. *J Thromb Haemost.* 2011; 9(5):1093-1095.
17. Friedman PA, Shia M. Some characteristics of a vitamin K-dependent carboxylating system from rat liver microsomes. *Biochem Biophys Res Commun.* 1976;70(2):647-654.
18. Mack DO, Suen ET, Girardot JM, Miller JA, Delaney R, Johnson BC. Soluble enzyme system for vitamin K-dependent carboxylation. *J Biol Chem.* 1976;251(11):3269-3276.
19. Hodroge A, Matagrin B, Moreau C, et al. VKORC1 mutations detected in patients resistant to vitamin K antagonists are not all associated with a resistant VKOR activity. *J Thromb Haemost.* 2012;10(12):2535-2543.
20. Rishavy MA, Usubalieva A, Hallgren KW, Berkner KL. Novel insight into the mechanism of the vitamin K oxidoreductase (VKOR): electron relay through Cys43 and Cys51 reduces VKOR to allow vitamin K reduction and facilitation of vitamin K-dependent protein carboxylation. *J Biol Chem.* 2011;286(9):7267-7278.
21. Bevans CG, Krettler C, Reinhart C, et al. Determination of the warfarin inhibition constant Ki for vitamin K 2,3-epoxide reductase complex subunit-1 (VKORC1) using an in vitro DTT-driven assay. *Biochim Biophys Acta.* 2013;1830(8): 4202-4210.
22. Fregin A, Czogalla KJ, Gansler J, et al. A new cell culture-based assay quantifies VKORC1 function and reveals warfarin resistance phenotypes not shown by the DTT-driven VKO assay. *J Thromb Haemost.* 2013;11(5):872-880.
23. Li W, Schulman S, Dutton RJ, Boyd D, Beckwith J, Rapoport TA. Structure of a bacterial homologue of vitamin K epoxide reductase. *Nature.* 2010;463(7280):507-512.
24. Unger T, Jacobovitch Y, Dantes A, Bernheim R, Peleg Y. Applications of the Restriction Free (RF) cloning procedure for molecular manipulations and protein expression. *J Struct Biol.* 2010;172(1): 34-44.
25. Morris GM, Goodsell DS, Halliday RS, et al. Automated docking using a Lamarckian genetic algorithm and an empirical binding free energy function. *J Comput Chem.* 1998;19(14): 1639-1662.
26. Krieger E, Koraimann G, Vriend G. Increasing the precision of comparative models with YASARA NOVA—a self-parameterizing force field. *Proteins.* 2002;47(3):393-402.
27. Krieger E, Darden T, Nabuurs SB, Finkelstein A, Vriend G. Making optimal use of empirical energy functions: force-field parameterization in crystal space. *Proteins.* 2004;57(4):678-683.
28. Krieger E, Joo K, Lee J, et al. Improving physical realism, stereochemistry, and side-chain accuracy in homology modeling: Four approaches that performed well in CASP8. *Proteins.* 2009; 77(Suppl 9):114-122.
29. Ma Q, Cui K, Xiao F, Lu AY, Yang CS. Identification of a glycine-rich sequence as an NAD(P)H-binding site and tyrosine 128 as a dicumarol-binding site in rat liver NAD(P)H: quinone oxidoreductase by site-directed mutagenesis. *J Biol Chem.* 1992;267(31): 22298-22304.
30. Asher G, Dym O, Tsvetkov P, Adler J, Shaul Y. The crystal structure of NAD(P)H quinone oxidoreductase 1 in complex with its potent inhibitor dicoumarol. *Biochemistry.* 2006;45(20): 6372-6378.
31. Myszka DG, Swenson RP. Synthesis of 3-(4-azido-5-iodosalicylamido)-4-hydroxycoumarin: photoaffinity labeling of rat liver dicoumarol-sensitive NAD(P)H: quinone reductase. *Biochem Biophys Res Commun.* 1990;172(2):415-422.
32. Gebauer M. Synthesis and structure-activity relationships of novel warfarin derivatives. *Bioorg Med Chem.* 2007;15(6):2414-2420.
33. Rost S, Fregin A, Hünerberg M, Bevans CG, Müller CR, Oldenburg J. Site-directed mutagenesis of coumarin-type anticoagulant-sensitive VKORC1: evidence that highly conserved amino acids define structural requirements for enzymatic activity and inhibition by warfarin. *Thromb Haemost.* 2005;94(4): 780-786.
34. Jin DY, Tie JK, Stafford DW. The conversion of vitamin K epoxide to vitamin K quinone and vitamin K quinone to vitamin K hydroquinone uses the same active site cysteines. *Biochemistry.* 2007;46(24):7279-7283.
35. Schulman S, Wang B, Li W, Rapoport TA. Vitamin K epoxide reductase prefers ER membrane-anchored thioredoxin-like redox partners. *Proc Natl Acad Sci USA.* 2010; 107(34):15027-15032.
36. Tie JK, Jin DY, Tie K, Stafford DW. Evaluation of warfarin resistance using transcription activator-like effector nucleases-mediated vitamin K epoxide reductase knockout HEK293 cells. *J Thromb Haemost.* 2013;11(8):1556-1564.
37. Tie JK, Jin DY, Stafford DW. Human vitamin K epoxide reductase and its bacterial homologue have different membrane topologies and reaction mechanisms. *J Biol Chem.* 2012;287(41): 33945-33955.
38. Tie JK, Nicchitta C, von Heijne G, Stafford DW. Membrane topology mapping of vitamin K epoxide reductase by in vitro translation/cotranslocation. *J Biol Chem.* 2005;280(16):16410-16416.
39. Van Horn WD. Structural and functional insights into human vitamin K epoxide reductase and vitamin K epoxide reductase-like1. *Crit Rev Biochem Mol Biol.* 2013;48(4):357-372.
40. Ernster L, Danielson L, Ljunggren M. DT diaphorase. I. Purification from the soluble fraction of rat-liver cytoplasm, and properties. *Biochim Biophys Acta.* 1962;58:171-188.